SECTION 1

INTRODUCTION

Seismic isolation is a relatively old concept that in recent years is being rapidly accepted throughout the world due to current advances in seismic isolation technology. The concept of seismic isolation (or base isolation) is based on the ability to provide a discontinuity between the structure and foundation. This discontinuity decouples the ground vibrations from the structure, causing a reduced level of response than would have been obtained from a fixed-base structure.

By decoupling the structure from the foundation, the lateral accelerations are reduced and hence the lateral forces are reduced. This decoupling is produced by the introduction of flexibility to the isolated structure. This flexibility shifts the fundamental period of the isolated structure to a period higher than the predominant periods of the seismic excitation. At this higher period, the response accelerations are significantly lower than the response accelerations at the fixed-base period. A consequence of the increased flexibility is an increase in the displacement of the system. This displacement needs to be controlled within acceptable design limits through damping or energy dissipating mechanisms.

Conventional fixed-base structures must resist seismic lateral forces through inelastic deformation of the structural system. Inelastic deformation causes an increase in the natural period of the structure and its ability to dissipate energy. The combined result of these effects is a reduction of inertia forces at the expense of damage to the structural system and to the non-structural components, including possible human injury. This damage can lead to liability suits and very costly repairs or demolition and rebuild costs.

The option of providing an isolation system can significantly reduce costs associated with earthquakes. The isolation system can be designed to limit the inelastic response to the isolation elements and therefore allow the structure to be designed as an elastic or nearly elastic system. Since the isolation system reduces the forces transmitted to the superstructure, the components of the superstructure may generally be designed for less force than the components of the same structure without an isolation system. This would result in lower initial construction costs and may help justify the increased costs involved with implementing an isolation system. Overall, and accounting for the reduction or elimination of costs associated with damage following an earthquake, seismic isolation offers a lower life-cycle cost.

Since conventional building design codes do not readily apply to isolated structures, the need for a specific document addressing the issues involving seismic isolated buildings became apparent in the early 1980's. As a result, the Southern and Northern sections of the Structural Engineers Association of California (SEAOC) published papers and recommended design guidelines for seismic isolated buildings in the mid 1980's (SEAONC, 1986). In order to compile all the research into a single document, the seismology committee of SEAOC developed "Tentative General Requirements for the Design and Construction of Seismic Isolated Structures" (SEAOC, 1990a) as an appendix to the "SEAOC Recommended Lateral Force Requirements" (SEAOC, 1990b). In 1991, the International Conference of Building Officials adopted the requirements and included them in the 1991 Uniform Building Code (ICBO, 1991). Furthermore, in June 1991, the American Association of State Highway and Transportation Officials (AASHTO) incorporated similar provisions for the design of bridge seismic isolation systems in the document "Guide Specifications for Seismic Isolation Design" (AASHTO, 1991).

These documents incorporate the most up to date research, experience, and information available so that design engineers and building officials have a set of guidelines for preparing, reviewing and enforcing regulations for isolated building design. As experience and the results of current research become available, the codes can be modified to incorporate new information regarding the behavior of isolated buildings. Presently, the codes require dynamic analysis for virtually all isolated buildings, but also provide simple equations that are considered conservative, to provide lower bound limits for the parameters calculated in the dynamic analysis.

The validity of the SEAOC/UBC static analysis procedure has been investigated by Kircher and Lashkari (1989). Kircher and Lashkari analyzed a rigid superstructure on a grid of 45 isolators with 31 different bilinear hysteretic properties using a comprehensive collection of 29 pairs of horizontal earthquake motions. The isolation system properties covered the entire range of interest in seismic isolation, that is, effective periods of 1 to 4 seconds and effective damping of 6% to 39% of critical. In general, the study confirmed the validity of the static analysis procedure on the determination of the isolation system displacement.

The study of Kircher and Lashkari (1989) neglected the following effects:

1. Superstructure flexibility. This prevented the calculation of shear force distributions in the superstructure.
2. Bi-directional interaction effects in the isolation bearings. For hysteretic softening systems, the neglect of this interaction typically results in underestimation of the isolation system displacement (Mokha, 1993). The amount of underestimation is greatest in systems with high characteristic strength and low stiffness.
3. The bilinear hysteretic models used did not strictly apply to frictional systems since they all had a yield displacement of 0.5 inches.

The constraints of the Kircher and Lashkari study have been relaxed in a subsequent study of Theodossiou and Constantinou (1991) which concentrated on sliding isolation systems. This study follows the approach established in the study of Theodossiou and Constantinou (1991), but concentrates on the same generic bilinear hysteretic isolation systems as the study of Kircher and Lashkari (1989).

The study provides a set of nonlinear time history analysis results using the comprehensive collection of 29 pairs of components in the Kircher and Lashkari (1989) study and a set of linear response spectrum analysis results. The response spectrum results and the SEAOC/UBC static analysis limits on bearing displacements and shear force distribution are compared to the results of nonlinear time history analysis and conclusions are drawn.

SECTION 2

SEAOC/UBC DESIGN REQUIREMENTS FOR ISOLATED STRUCTURES

2.1 General Requirements

Since the design techniques of different seismic isolation systems vary, the SEAOC/UBC guidelines only provide general requirements and limits that are expected to prevent an unrealistic design. The design requirements allow the use of two different procedures for determining seismic design quantities. The first procedure is called the static analysis procedure and provides a simple method of calculating lower bound limits for design. The static analysis procedure may be used alone in a few cases, where the structure is located away from active faults, is relatively stiff, and is of regular configuration. For all other cases, the guidelines require the second procedure, a rigorous dynamic analysis procedure to determine response quantities.

2.2 Static Analysis Procedure

The SEAOC/UBC regulations specify the following design displacement for the isolation system:

$$D = \frac{10 Z N S_I T_I}{B} \tag{2.1}$$

where:

- D = Design displacement in inches at the center of rigidity of the isolation system in the direction under consideration.
- Z = Seismic Zone coefficient (Table 2-I)
- N = Near-field response coefficient (Table 2-II)
- S_I = Site coefficient for soil profile (Table 2-III)
- T_I = Period of isolated structure
- B = Effective damping coefficient (Table 2-IV)

The period of the isolated structure is given by

$$T_I = 2\pi \sqrt{\frac{W}{K_{min}\, g}} \tag{2.2}$$

where:

W = Total seismic dead load

K_{min} = Minimum effective stiffness of the isolation system

g = Acceleration due to gravity

TABLE 2-I Seismic Zone Coefficient Z

Seismic Zone	0	1	2A	2B	3	4
Z	0.05	0.1	0.15	0.2	0.3	0.4

TABLE 2-II Near-Field Response Coefficient N

Closest Distance, d_F to an Active Fault[1]	$d_F > 15$ km	$d_F = 10$ km	$d_F < 5$ km
N	1.0	1.2	1.5

[1]Coefficients other than those listed shall be based on linear interpolation.

TABLE 2-III Site Coefficient S_I

Soil Profile Type	S_1	S_2	S_3	S_4
S_I	1.0	1.5	2.0	2.7

TABLE 2-IV Coefficient B Related to Effective Damping

Effective Damping β (Percent of Critical)[1]	< 2%	5%	10%	20%	30%	40%	> 50%
B	0.8	1.0	1.2	1.5	1.7	1.9	2.0

[1]Coefficients other than those listed shall be based on linear interpolation.

The regulations specify a total design displacement, D_T, based on the geometrical dimensions of the base, that is intended to account for torsional displacement at the corner bearings:

$$D_T = D \left[1 + 12 \frac{ye}{b^2 + d^2} \right] \tag{2.3}$$

in which e = eccentricity, y = distance between the center of isolation system rigidity and the point of interest, b and d = plan dimensions of the structure.

For verification of the isolation system stability, the regulations require that the bearings be designed for a displacement 50% larger than this total design displacement, D_T. This displacement is called the total maximum design displacement, D_{TM}, and is defined as the displacement, including torsion, in the maximum credible earthquake:

$$D_{TM} = 1.5 D_T \tag{2.4}$$

The regulations specify the design base shear, V_b, at or below the isolation interface that corresponds to the design displacement:

$$V_b = \frac{K_{max} D}{1.5} \tag{2.5}$$

where K_{max} = maximum effective stiffness of the isolation system. The factor of 1.5 is used to approximate the relation between nominal strength and design allowables. For elements above the isolation interface, the regulations specify the following minimum shear force, V_S, and interstory drift ratios:

$$V_S = \frac{K_{\max} D}{R_{WI}} \tag{2.6}$$

$$\max \; \textit{interstory drift ratio} \;\leq\; \frac{0.010}{R_{WI}} \tag{2.7}$$

where R_{WI} is a reduction factor based on the type of structural system.

The distribution of forces over the height of the structure is specified by

$$F_X = \frac{V_S \, w_x}{\sum_{i=1}^{n} w_i} \tag{2.8}$$

where w_i, w_x represent the portion of total seismic dead load assigned to level i or x. Inherent in equation (2.8) is the assumption of constant acceleration over the entire height of the isolated structure.

2.3 Dynamic Analysis Procedure

2.3.1 Conditions for Use

The dynamic analysis procedure is classified as time history analysis or as response spectrum analysis. The time history analysis is the most rigorous analysis procedure since linear or nonlinear behavior can be modeled, while for response spectrum analysis, only linear systems or equivalent linear systems can be modeled. The dynamic analysis procedure is required for design of the following structures:

1 The structure is located within 15 km of an active fault.

2. The structure is located on a soil profile with a site factor S_3 or S_4 (soft or very soft soils).
3. The structure is located in seismic zone number 0, 1, 2A, or 2B.
4. The structure above the isolation interface is greater than 4 stories or 65 feet, in height.
5. The isolated period of the structure is greater than 3 seconds.
6. The isolated period of the structure is less than 3 times the elastic fixed-base period of the structure above the isolation system.
7. The structure above the isolation system is of irregular configuration.

Furthermore, a time history analysis is required under the following conditions:

1. The structure is located on a soil profile with a site factor S_4.
2. The isolation system limits the maximum credible earthquake displacement to less than 1.5 times the design-basis earthquake displacement.
3. The effective stiffness of the isolation system at the design displacement is less than one third of the effective stiffness at 20 percent of the design displacement.
4. The isolation system is not capable of producing a restoring force at the total design displacement of at least 0.025W greater than the lateral force at 50% of the total design displacement.
5. The isolation system has force-deflection properties which are dependent of the rate of loading or dependent of vertical load and bilateral load.

2.3.2 Response Spectrum Analysis

The regulations specify that the response spectrum analysis shall be performed using a damping value equal to the effective damping of the isolation system or 30 percent of critical, whichever is less. Response spectrum analysis used to determine the total design displacement and the total maximum displacement must include simultaneous excitation of the model by 100 percent of the most critical direction of ground motion and 30 percent of the ground motion on the orthogonal axis.

Isolated structures with an isolated period, T_I greater than 3.0 seconds, or located on a soil type profile of S_3 or S_4, or located within 15 km of an active fault or located in Seismic Zone No. 1, 2A or 2B require properly substantiated, site-specific spectra for design. The regulations specify that all other isolated structures not requiring site-specific spectra be designed using response spectra based on spectral shapes of Figure 2-1. These design spectra must not be taken as less than the normalized response spectra given in Figure 2-1 for the appropriate soil type, scaled by the seismic zone coefficient.

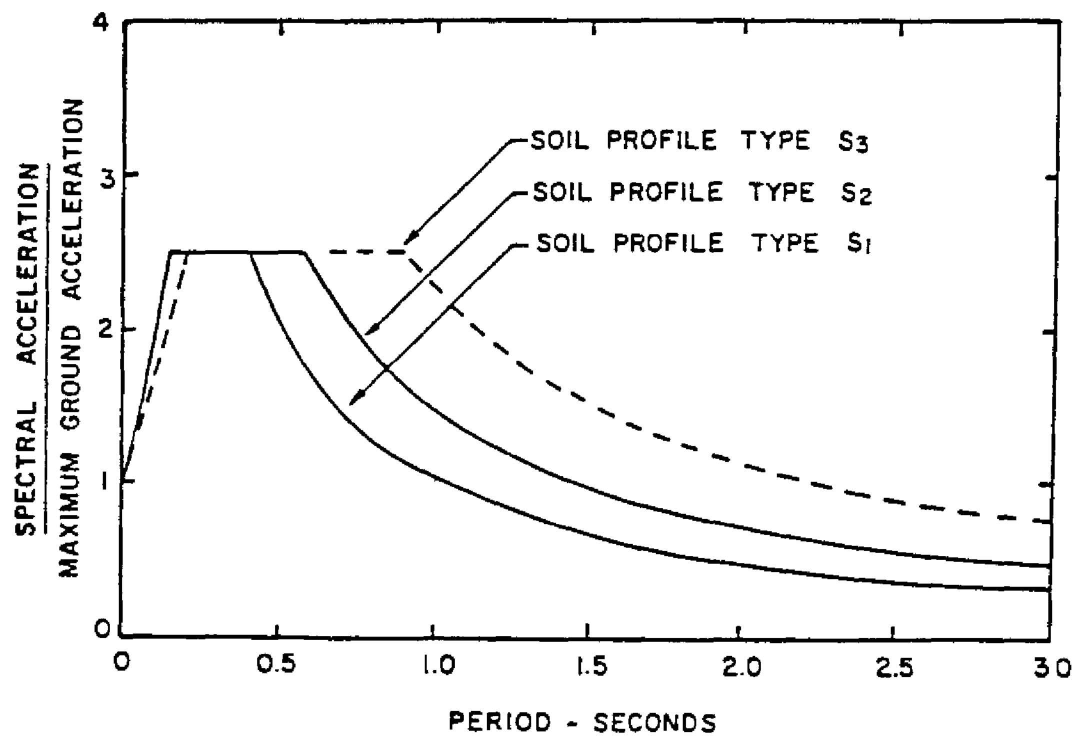

FIGURE 2-1 Normalized Uniform Building Code Response Spectra Shapes

2.3.3 Time History Analysis

The regulations specify that time history analysis be performed with pairs of horizontal ground motion time-history components, selected from at least three recorded events. These motions must be scaled such that the square root sum of the squares (SRSS) of their 5-percent damped spectra does not fall below 1.3 times the 5-percent damped spectrum of the design basis earthquake by more than 10 percent in the period range of T_I, as determined by equation (2-2), for periods from T_I minus 1.0 seconds to T_I plus 2.0 seconds. The duration of the time histories must be consistent with the magnitude and source characteristics of the design basis earthquake (or maximum credible earthquake). Time histories developed for sites within 15 km of a major active fault must incorporate near-fault phenomena. The maximum response of the parameter of interest calculated by the three time history analyses must be used for design.

The time history analysis must account for the following in detail:

1. Spatial distribution of isolators.
2. Torsional effects.
3. Effect of overturning/uplift forces.
4. Effects of vertical load, rate of loading and bi-directional interaction on the force-deflection properties of the isolators.

2.3.4 Lower Bound Limits for Dynamic Analysis Procedure

Certain lower bound limits confine the response values obtained through a dynamic analysis procedure. When the factored lateral shear force on structural elements, determined using either response spectrum analysis or time history analysis, is less than the lower bound limits, then all response parameters, including member forces and moments must be adjusted upward proportionally. The lower bound limits are described below.

2.3.4.1 Isolation System and Structural Elements Below the Isolation Interface

1. The total design displacement of the isolation system shall not be taken as less than 90 percent of D_T as specified by equation (2.3).
2. The total maximum displacement of the isolation system shall not be taken as less than 80 percent of D_{TM} as specified by equation (2.4).
3. The design lateral shear force on the isolation system and structural elements below the isolation interface shall not be taken as less than 90 percent of V_b as prescribed by equation (2.5).

2.3.4.2 Structural Elements Above the Isolation Interface

1. The design lateral shear force on the structure above the isolation interface, if regular in configuration, shall not be taken as less than 80 percent of V_S as prescribed by equation (2.6), nor less than the limits listed below:
   a. The lateral seismic force of a fixed-base structure of the same weight, W, and a period equal to the isolated period, T_I.
   b. The base shear corresponding to the design wind load.
   c. The lateral seismic force required to fully activate the system (eg. yield level of a softening system, ultimate capacity of a sacrificial wind-restraint system or the static friction level of a sliding system).

   EXCEPTION: The design lateral shear force on the structure above the isolation interface, if regular in configuration, may be taken as less than 80 percent of V_S, but not less than 60 percent of V_S, when time history analysis is used for design of the structure.

2. The design lateral shear force on the structure above the isolation interface, if irregular in configuration, shall not be taken as less than V_S as prescribed by equation (2.6), nor less than the limits listed above in 1a, 1b and 1c.

EXCEPTION: The design lateral shear force on the structure above the isolation interface, if irregular in configuration, may be taken as less than V_S, but not less than 80 percent of V_S, when time history analysis is used for design of the structure

2.3.4.3 Drift Limits

Maximum interstory drift corresponding to the design lateral force must not exceed the following limits:

1. The maximum interstory drift ratio of the structure above the isolation system, calculated by response spectrum analysis, shall not exceed $0.015/R_{WI}$.
2. The maximum interstory drift ratio of the structure above the isolation system, calculated by time history analysis considering the force-deflection characteristics of nonlinear elements of the lateral force resisting system, shall not exceed $0.020/R_{WI}$.
3. The secondary effects of the maximum credible earthquake lateral displacement (delta) of the structure above the isolation system combined with gravity forces shall be investigated if the interstory drift ratio exceeds $0.010/R_{WI}$.

SECTION 3

MODELS OF STRUCTURE AND ISOLATION SYSTEM

3.1 Introduction

The study of Kircher and Lashkari (1989) established a procedure for evaluating the SEAOC/UBC regulations. In this procedure, a comprehensive collection of 29 pairs of scaled earthquake motions are used in time history analyses of an isolated structure supported by 45 isolators. The earthquake motions are representative of Seismic Zone 4 and soil conditions S_1 or S_2. The results of the time history analyses are used to obtain statistical response quantities for comparison to the results obtained by the procedures of the SEAOC/UBC regulations.

This study follows the procedure established by Kircher and Lashkari (1989) but accounts for the following which were neglected in the Kircher and Lashkari study:

1. Flexibility of the superstructure, and
2. Bi-directional interaction effects at the isolation bearings.

In this way, a new collection of nonlinear time history analysis results is created for comparison to the results obtained by the static and response spectrum analysis procedures of SEAOC/UBC. This new collection of results includes data on the distribution of shear force over the height of isolated structures. Furthermore, the new collection of results on the bearing displacements is considered more accurate than the results of Kircher and Lashkari (1989) because they were obtained with a more realistic model of the isolation system. A description of the superstructure and isolation system models, together with the results on the effects of bi-directional interaction are presented in the succeeding sections.

3.2 Superstructure Configuration

The superstructure models used in this study were representative of one and eight story moment resisting frames. The plan view of the structure (shown in Figure 3-1) consisted of four bays by eight bays, creating a rectangular configuration. Each bay was square, measuring 20 feet by 20 feet. The height of all stories was 12 feet.

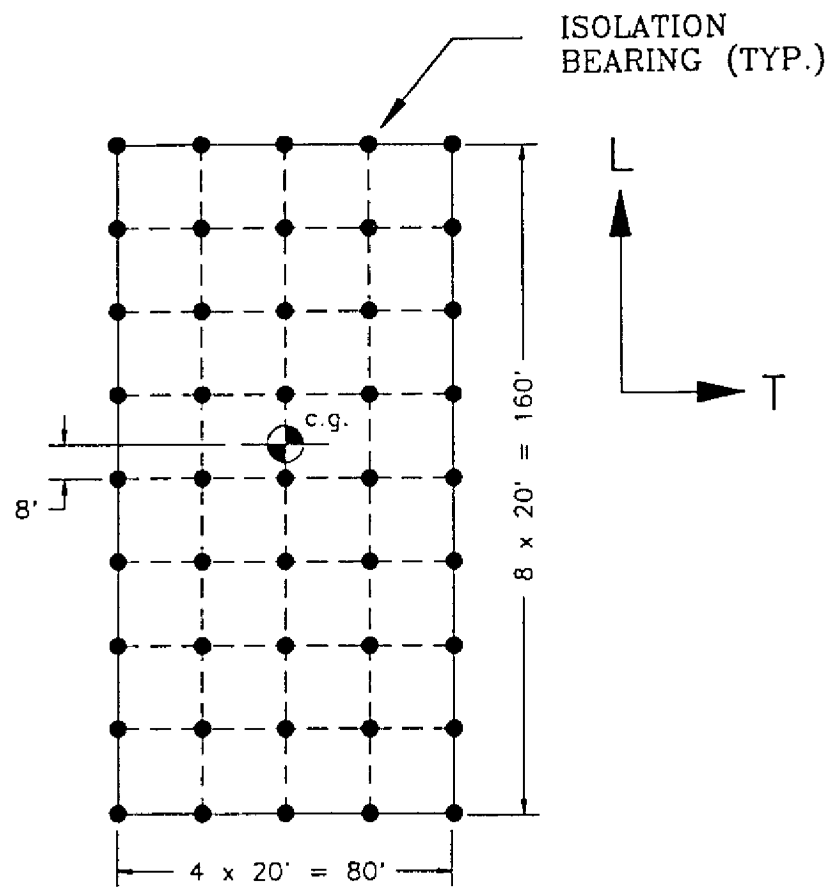

Figure 3-1 Plan View of the Base of the Building Models and Location of the Isolation Bearings

Both the 1-story and the 8-story superstructures had equal stiffnesses in the transverse and longitudinal directions. In the 8-story superstructure, the first three stories had the same stiffness, the next three stories had 0.75 times the stiffness of the first three stories and the top two stories had half the stiffness of the first three stories. The weight of each floor was 1280 kips (based on dead plus seismic live load of 100 psf). This created a total weight (including the base) of 2560 kips for the 1-story superstructure and 11520 kips for the 8-story superstructure. The mass on each floor, including the base, was asymmetric so that an eccentricity of 5% of the longest plan dimension (longitudinal) was created.

The horizontal stiffness and weight of the superstructure created a fundamental period of 0.2 seconds for the 1-story fixed-base superstructure and of 1.14 seconds for the 8-story fixed-base superstructure under elastic conditions. These values are representative of moment resisting type frames with the heights used. The distribution of stiffnesses to the columns was selected in such way as to result in a torsional period of 0.58 times the translational period, in the absence of eccentricities.

The properties of the 1-story and 8-story superstructures are tabulated in Tables 3-I and 3-II, respectively. The free vibrational dynamic characteristics of the two fixed-base superstructure systems are listed in Tables 3-III and 3-IV. They were obtained in dynamic analysis of the systems based on a shear type representation with three degrees of freedom per floor. The fundamental period of the two structures in the transverse direction is slightly larger than 0.2 seconds and 1.14 seconds because of the effect of the mass eccentricity in the longitudinal direction. The dynamic characteristics of the 8-story superstructure account for nine out of twenty four modes. The contribution of the higher modes was assumed insignificant since they correspond to periods of less than 0.19 seconds.

3.3 Isolation Systems

Since most commercially available isolation systems (softening systems) can be reasonably well modeled by bilinear behavior, the nonlinear force-deflection characteristics of the isolation systems used in this study were modeled by bilinear hysteretic elements. These isolation systems used, were identical to the systems analyzed in the Kircher and Lashkari (1989) study. Specific isolation systems were selected for this study that were applicable to only S_1 and S_2 type (stiff

TABLE 3-I Properties for 1-story Structure

Story / Floor	Weight (Kips)	Rotational Inertia (Kips-in-sec^2)	Stiffness (Kips/in)	Rotational Stiffness (Kips-in)	Eccentricity (ft)	
					Longitudinal	Transverse
1	1280	1272642.5	3271.0	3733792620	8	0
Base	1280	1272642.5			8	0

TABLE 3-II Properties for 8-story Structure

Story / Floor	Weight (Kips)	Rotational Inertia (Kips-in-sec^2)	Stiffness (Kips/in)	Rotational Stiffness (Kips-in)	Eccentricity (ft)	
					Longitudinal	Transverse
8	1280	1272642.5	1700.9	1997933760	8	0
7	1280	1272642.5	1700.9	1997933760	8	0
6	1280	1272642.5	2551.3	2996900640	8	0
5	1280	1272642.5	2551.3	2996900640	8	0
4	1280	1272642.5	2551.3	2996900640	8	0
3	1280	1272642.5	3401.8	3995867520	8	0
2	1280	1272642.5	3401.8	3995867520	8	0
1	1280	1272642.5	3401.8	3995867520	8	0
Base	1280	1272642.5			8	0

TABLE 3-III Dynamic Characteristics of 1-story Superstructure (Including 5 % mass Eccentricity)

Floor	Mode								
	1			2			3		
	L Component	T Component	Rotational Component	L Component	T Component	Rotational Component	L Component	T Component	Rotational Component
1	0.000	0.547	6.898 E-05	0.549	0.000	0.000	0.000	-0.0427	8.837 E-04

Period (sec)	0.201	0.200	0.116
Frequency (Hz)	4.970	4.998	8.637
Modal damping ratio	0.03	0.03	0.03

TABLE 3-IV Dynamic Characteristics of 8-story Superstructure (Including 5 % mass Eccentricity)

Floor	Mode								
	1			2			3		
	L Component	T Component	Rotational Component	L Component	T Component	Rotational Component	L Component	T Component	Rotational Component
8	0.000	0.285	3.440 E-05	0.286	0.000	0.000	0.000	-0.0213	4.598 E-04
7	0.000	0.268	3.237 E-05	0.269	0.000	0.000	0.000	-0.0200	4.326 E-04
6	0.000	0.235	2.842 E-05	0.236	0.000	0.000	0.000	-0.0176	3.798 E-04
5	0.000	0.204	2.466 E-05	0.205	0.000	0.000	0.000	-0.0153	3.296 E-04
4	0.000	0.165	1.993 E-05	0.166	0.000	0.000	0.000	-0.0124	2.664 E-04
3	0.000	0.119	1.442 E-05	0.120	0.000	0.000	0.000	-0.0089	1.927 E-04
2	0.000	0.082	0.986 E-05	0.082	0.000	0.000	0.000	-0.0061	1.317 E-04
1	0.000	0.041	0.500 E-05	0.042	0.000	0.000	0.000	-0.0031	0.668 E-04

Period (sec)	1.147	1.140	0.651
Frequency (Hz)	0.872	0.877	1.537
Modal damping ratio	0.03	0.03	0.03

TABLE 3-IV Continued

Floor	Mode 4			Mode 5			Mode 6		
	L Component	T Component	Rotational Component	L Component	T Component	Rotational Component	L Component	T Component	Rotational Component
8	0.000	-0.290	-3 505 E-05	-0.291	0 000	0 000	0 000	0 236	2.850 E-05
7	0.000	-0.165	-1 989 E-05	-0 166	0.000	0.000	0.000	-0.023	-0.279 E-05
6	0 000	0.032	0 386 E-05	0.032	0.000	0.000	0.000	-0.257	-3.101 E-05
5	0.000	0 154	1 858 E-05	0.154	0.000	0 000	0 000	-0.225	-2 713 E-05
4	0.000	0.231	2.795 E-05	0.232	0.000	0 000	0 000	-0.028	-0 034 E-05
3	0 000	0.242	2 926 E-05	0.243	0.000	0.000	0 000	0.189	2.283 E-05
2	0 000	0.198	2.392 E-05	0.199	0.000	0.000	0 000	0 248	2.996 E-05
1	0.000	0.111	1 341 E-05	0.111	0.000	0.000	0 000	0 171	2 065 E-05

	Mode 4	Mode 5	Mode 6
Period (sec)	0.424	0 422	0.266
Frequency (Hz)	2.357	2.371	3.756
Modal damping ratio	0.03	0.03	0 03

TABLE 3-IV Continued

Floor	Mode 7			Mode 8			Mode 9		
	L Component	T Component	Rotational Component	L Component	T Component	Rotational Component	L Component	T Component	Rotational Component
8	0.237	0.000	0 000	0.000	0.022	-4.684 E-04	0.000	-0.223	-2.692 E-05
7	-0 023	0.000	0 000	0.000	0 012	-2.659 E-04	0.000	0 254	3.063 E-05
6	-0.258	0.000	0.000	0.000	-0.002	-0.516 E-04	0.000	0.188	2.270 E-05
5	-0 225	0.000	0.000	0.000	-0.012	2.483 E-04	0 000	-0.124	-1 493 E-05
4	-0 028	0.000	0.000	0.000	-0.017	3.735 E-04	0 000	-0.259	-3.129 E-05
3	0 189	0.000	0 000	0.000	-0.018	3.911 E-04	0 000	-0.025	-0.305 E-05
2	0.249	0.000	0 000	0.000	-0 015	3 197 E-04	0 000	0.177	2.138 E-05
1	0.171	0.000	0 000	0.000	-0 008	1.792 E-04	0.000	0.190	2 297 E-05

	Mode 7	Mode 8	Mode 9
Period (sec)	0.265	0.241	0 191
Frequency (Hz)	3.778	4.154	5 241
Modal damping ratio	0.03	0.03	0.03

and medium) soils. Each isolation system had a different "characteristic" strength (or yield force) and post yielding stiffness in order to create a set of isolation schemes that range from almost linear to highly nonlinear. It is expected that these isolated building models would represent the dynamic characteristics of a significant portion of feasible isolation schemes.

The idealized bilinear hysteretic model of the isolation systems is shown in Figure 3-2. The model is characterized by the initial and unloading stiffness, K_1, the post-yielding stiffness, K_2, the yield force, F_y and the yield displacement, D_y. For a particular displacement amplitude, D, the isolation system may be described by equivalent linear-viscous properties in accordance with the SEAOC/UBC guidelines. These properties are the effective period, T_I, given by equation (2.2) with K_{min} equal to K_{eff} and the effective damping ratio, β

$$\beta = \frac{W_D}{2\pi K_{eff} D^2} \tag{3.1}$$

where W_D = area enclosed by the hysteresis loop.

The analyzed isolation systems were selected from Kircher and Lashkari (1989). All had a yield displacement D_y = 0.5 in. Their force-displacement characteristics are depicted in Figures 3-3 and 3-4. Their nonlinear properties and equivalent linear properties are given in Tables 3-V and 3-VI. The equivalent linear properties are based on the design displacement, D, as calculated by the static analysis procedure of SEAOC/UBC. It may be seen that the properties of the analyzed isolation systems cover the period range of 1.5 to 3 secs and the effective damping range of 6 to 39% of critical.

3.4 Nonlinear Time History Analysis

Nonlinear time history analyses were performed with computer code 3D-BASIS (Nagarajaiah et al, 1991). Each of the 45 isolators was explicitly modeled by a smooth bilinear hysteretic element with bi-directional interaction capability. All 45 isolators had identical properties.

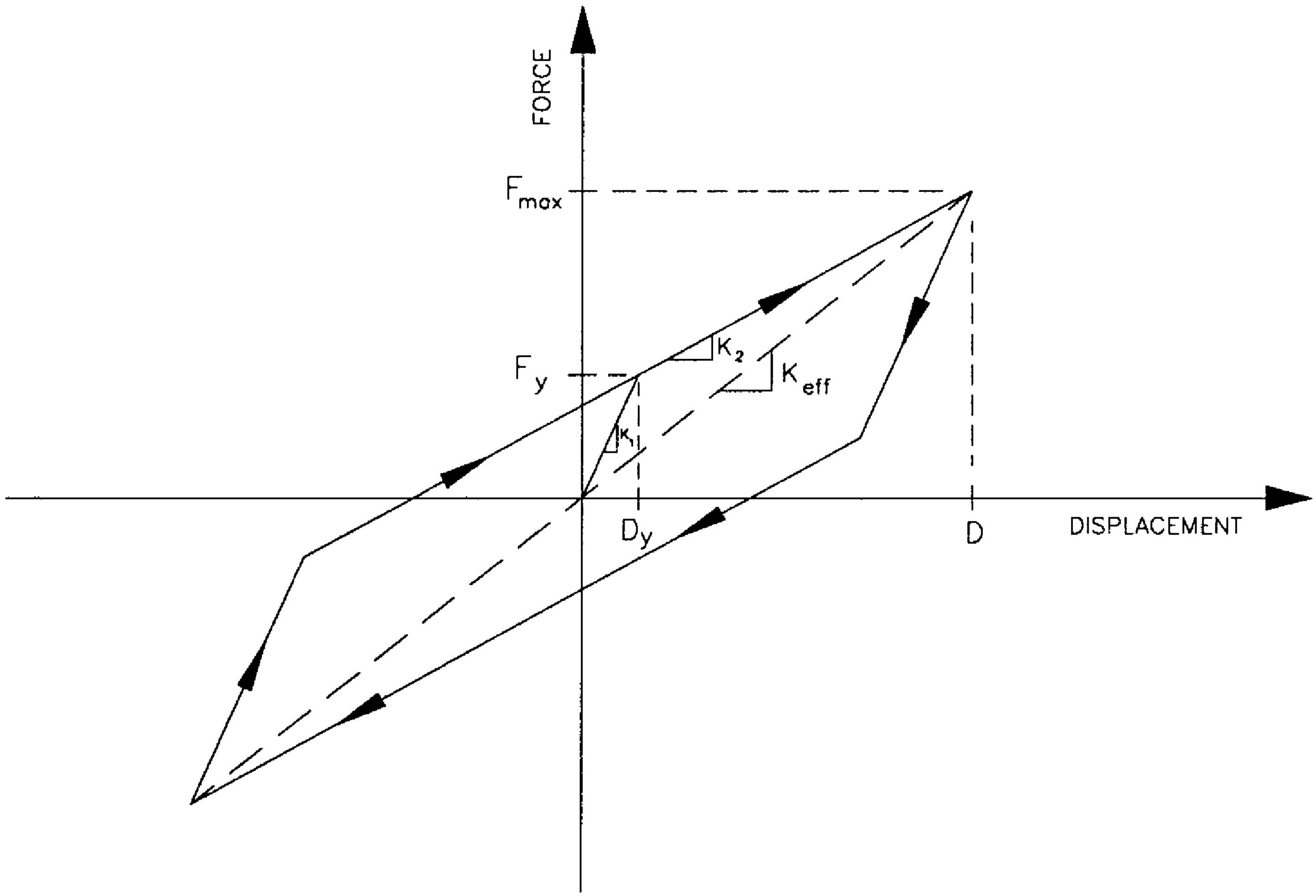

FIGURE 3-2 Idealized Properties of the Isolation Systems

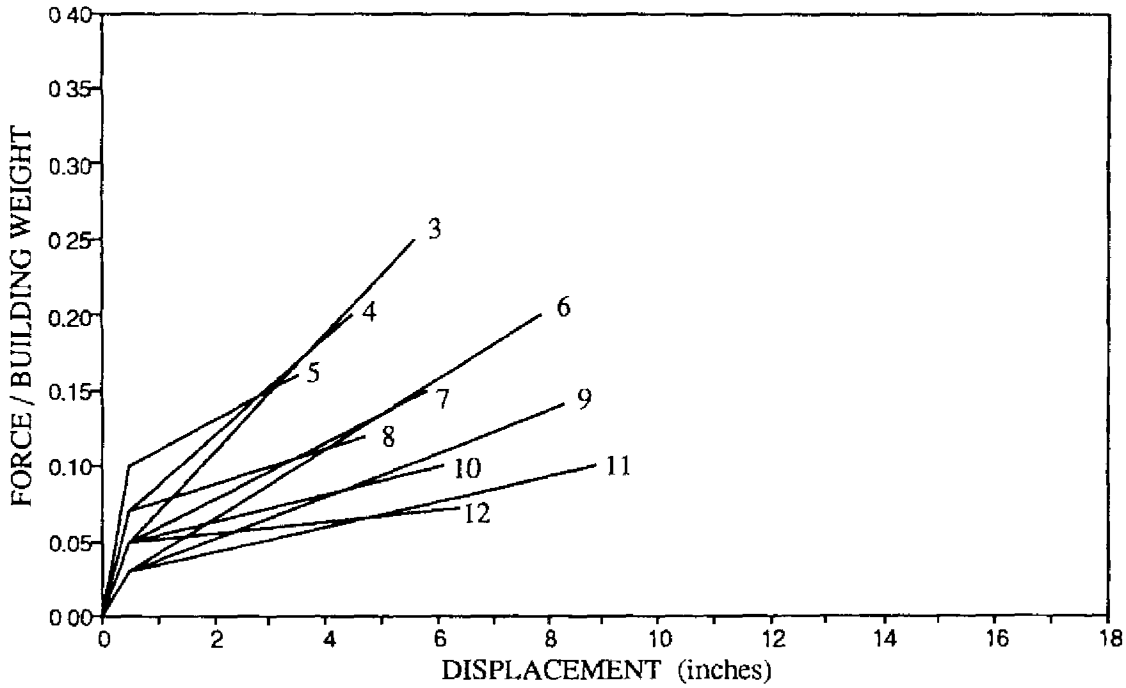

FIGURE 3-3 Force-Displacement Characteristics of the Isolation Systems Analyzed on Stiff Soil Sites

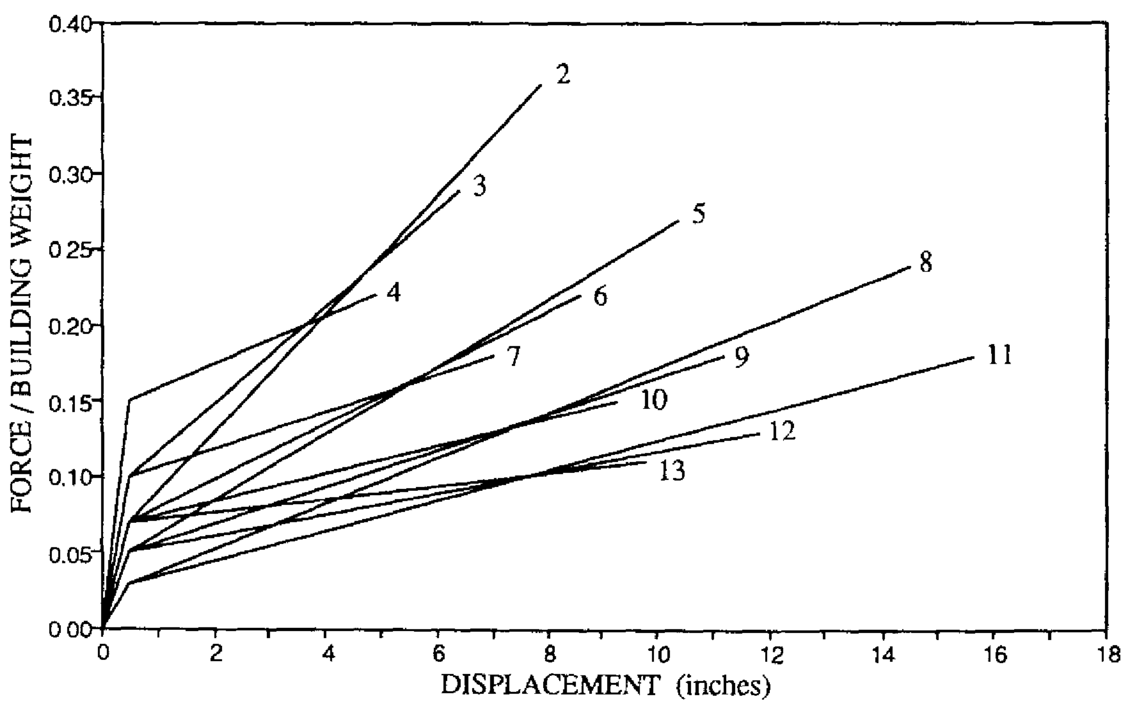

FIGURE 3-4 Force-Displacement Characteristics of the Isolation Systems Analyzed on Medium Soil Sites

TABLE 3-V Properties of Isolation Systems Analyzed on Stiff Soil Profiles (S_1)

Isolation System Type Number	Equivalent Linear Properties		Design Parameters		Parameters in Nonlinear Analysis		
	Period (sec)	Damping Ratio (%)	D (inches)	$\frac{F_{max}}{W}$	$\frac{\text{YIELD FORCE}}{W}$	D_y (inches)	$\alpha = \frac{K_2}{K_1}$
3	1.5	7	5.6	0.25	0.05	0.5	0.39216
4	1.5	15	4.5	0.20	0.07	0.5	0.23214
5	1.5	31	3.5	0.16	0.10	0.5	0.10000
6	2.0	6	7.9	0.20	0.03	0.5	0.38288
7	2.0	16	5.8	0.15	0.05	0.5	0.18868
8	2.0	30	4.7	0.12	0.07	0.5	0.085034
9	2.5	10	8.3	0.14	0.03	0.5	0.23504
10	2.5	27	6.1	0.10	0.05	0.5	0.089286
11	3.0	16	8.9	0.10	0.03	0.5	0.13889
12	3.0	39	6.4	0.073	0.05	0.5	0.038983

TABLE 3-VI Properties of Isolation Systems Analyzed on Medium Soil Profiles (S_2)

Isolation System Type Number	Equivalent Linear Properties		Design Parameters		Parameters in Nonlinear Analysis		
	Period (sec)	Damping Ratio (%)	D (inches)	$\frac{F_{max}}{W}$	$\frac{\text{YIELD FORCE}}{W}$	D_y (inches)	$\alpha = \frac{K_2}{K_1}$
2	1.5	8	7.9	0.36	0.07	0.5	0.27992
3	1.5	17	6.4	0.29	0.10	0.5	0.16102
4	1.5	37	4.9	0.22	0.15	0.5	0.053030
5	2.0	9	10.4	0.27	0.05	0.5	0.22222
6	2.0	17	8.6	0.22	0.07	0.5	0.13228
7	2.0	31	7.0	0.18	0.10	0.5	0.061538
8	2.5	6	14.5	0.24	0.03	0.5	0.25000
9	2.5	15	11.2	0.18	0.05	0.5	0.12150
10	2.5	26	9.3	0.15	0.07	0.5	0.064935
11	3.0	9	15.7	0.18	0.03	0.5	0.16447
12	3.0	22	11.8	0.13	0.05	0.5	0.070796
13	3.0	37	9.8	0.11	0.07	0.5	0.030722

The model of isolation bearings in this study differed from the model used by Kircher and Lashkari (1989) in the following aspects. First, the transition from elastic to the post-yielding range is smooth rather than abrupt. Second, the forces in the two orthogonal directions of each bearing exhibit circular interaction. The significance of these differences is investigated next.

3.4.1 Comparison of Smooth 3D-BASIS Model and Idealized Bilinear Hysteretic Model for Isolation Bearings

The idealized bilinear hysteretic model shown in Figure 3-2, exhibits an abrupt change from elastic to post-yielding stiffness at displacements equal to D_y and $(D - 2D_y)$. The actual behavior of elastomeric isolation bearings is rather different. The change in stiffness occurs smoothly over a finite displacement interval. This smooth transition between the two stages is realistically modeled in computer code 3D-BASIS.

In order to investigate the significance of this difference in modeling bilinear hysteretic behavior, analyses were performed with the smooth and the idealized bilinear hysteretic models. To avoid masking the results, the superstructure of the isolated system was considered rigid and the excitation was applied in only the longitudinal (L) direction so that the response occurred in only that direction. Note that mass eccentricity exists only in the longitudinal direction (see Figure 3-1).

Isolation system type No. 7 (T_I = 2.0 secs, β = 31%) for medium soil type (S_2) was analyzed with excitation being the components No. 25-T and No. 26-T of the scaled earthquake motions used in the nonlinear time history analyses (see Table 4-II for details). A comparison of responses obtained by the two models is shown in Figures 3-5 and 3-6. Evidently, the hysteresis loops trace nearly identical paths with only very small difference in the calculated peak response.

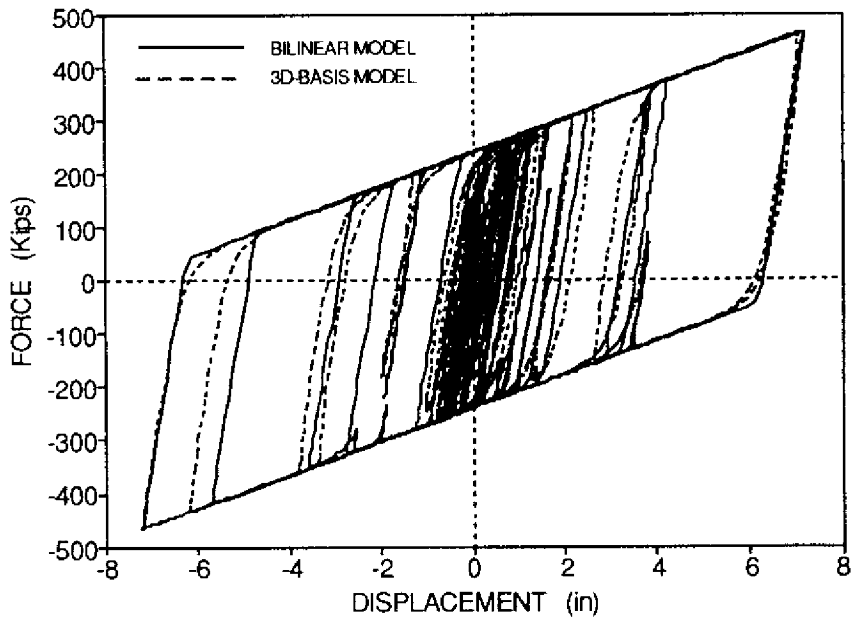

FIGURE 3-5 Force-Displacement Loops for Isolation System Type No. 7 (T_I = 2.0 sec, β = 31%), Soil Type S_2, Excitation No. 25 San Fernando (241) T-direction only

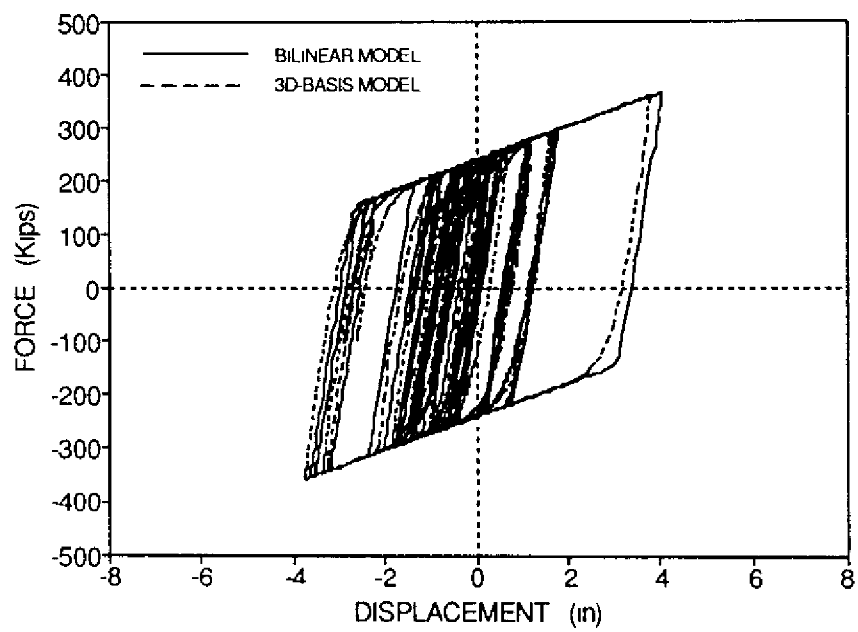

FIGURE 3-6 Force-Displacement Loops for Isolation System Type No. 7 (T_I = 2.0 sec, β = 31%), Soil Type S_2, Excitation No. 26 San Fernando (458) T-direction only

3.4.2 Comparison of Uniaxial and Biaxial Interaction Models for Isolation Bearings

The significance of the bi-directional interaction effect in sliding isolation bearings has been demonstrated by Mokha et al, (1993). In general, consideration of this effect results in larger bearing displacements. This conclusion is expected to hold true for all bilinear hysteretic (non-stiffening) isolation systems since they differ from sliding systems with restoring force in only the level of the yield displacement.

Figure 3-7 illustrates the differences between models of isolation bearings with and without bidirectional interaction. A valid model for isolation bearings should exhibit identical force-displacement characteristics in all directions, as it would have been the case for a circular rubber bearing. In this case, the yield surface (or curve) is circular. A model without due regard to the bi-directional interaction effects consists of two uniaxial bilinear hysteretic elements placed along the principal directions of the bearing. Effectively in this case, the yield surface is square as shown in Figure 3-7. The implications are apparent. For motion along a direction other than the two orthogonal ones, the yield force and yield displacement are larger than F_y and D_y, respectively. Effectively, the model without bidirectional interaction effects exhibits more characteristic strength. The result is a reduction in bearing displacement.

To demonstrate the significance of neglecting the bi-directional interaction effects, the 1-story isolated structure was analyzed with and without due regard for the bidirectional interaction effects. Analyses were performed for isolation system types No. 6, 8 and 12 on soil type S_1 and isolation system types No. 5, 7, 9 and 13 on soil type S_2 (see Tables 3-V and 3-VI). The excitation consisted of the collection of scaled pairs of earthquake motions as described in section 4. Detailed results for each earthquake motion and isolation system type are presented in Appendix A. Table 3-VII presents a summary of the results in terms of the mean and mean plus one standard deviation (σ) of the bearing displacements and structural shear force. It may be observed that bearing displacements in the case without bidirectional interaction are typically less (exception is system type No. 13, soil type S_2) than the case with bidirectional interaction effects.

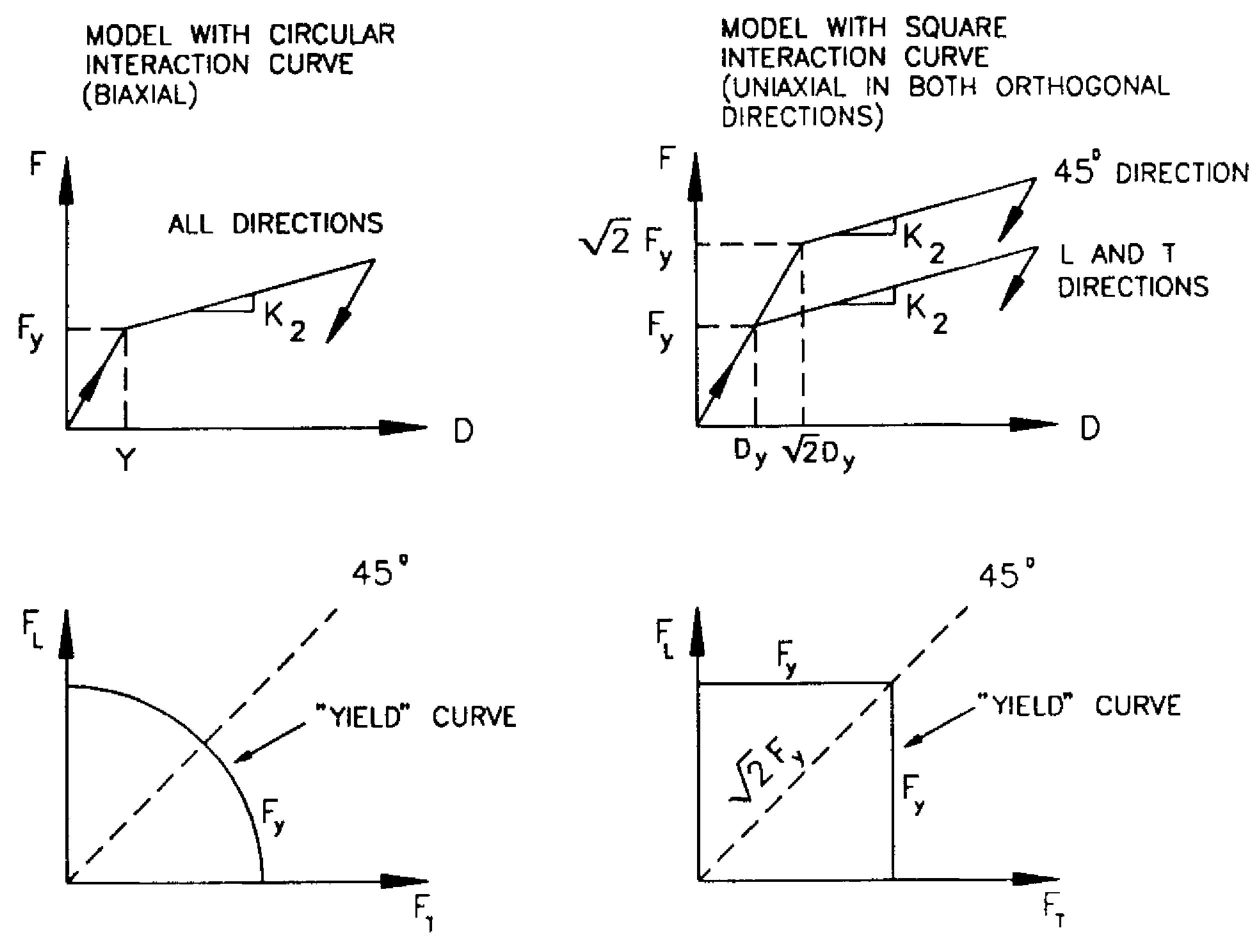

FIGURE 3-7 Comparison of Circular and Square Interaction Models of Isolation Bearings

TABLE 3-VII Comparison of Results of Time History Analyses with and without due Regard for Bidirectional Interaction Effects.

SOIL TYPE	ISOLATION TYPE No	BASE CENTER DISPL. (in)				CORNER BEARING DISPL. (in)				STRUCTURAL SHEAR / WEIGHT			
		MEAN		MEAN + 1 σ		MEAN		MEAN + 1 σ		MEAN		MEAN + 1 σ	
		WITH	W/OUT	WITH	W/OUT	WITH	W/OUT	WITH	W/OUT	WITH	W/OUT	WITH	W/OUT
S_1	6	8.97	8.34	10 73	9.50	10.71	9.89	13.00	11.47	0.108	0.104	0.129	0.117
	8	5.75	5.21	7.62	6 98	6.92	5.80	9 57	7.89	0.062	0.068	0.072	0.077
	12	9.63	8.74	13.92	12.34	11.21	9.70	16.85	13 93	0.042	0.044	0.048	0.049
S_2	5	12.86	12.07	18 20	17.18	14.74	13.85	20.76	19.88	0.156	0.155	0.214	0.210
	7	7.03	6.97	9.49	9 27	7.76	7.71	10.24	9.95	0.095	0.102	0.102	0.115
	9	13.27	12.47	20.29	18.37	14.87	13.90	22.16	20 27	0.096	0.099	0.137	0.134
	13	9.12	9.31	12.89	13.02	10.13	10.17	14.24	14.25	0 059	0.064	0.066	0.070

Differences as high as 18% demonstrate the significance of accounting for the bidirectional interaction effects.

3.5 Response Spectrum Analysis

Response spectrum analyses were performed with computer code ETABS (Wilson et al, 1975). The excitation was specified by the design spectrum with proper modification in order to account for the difference between the actual modal damping ratios in the isolated structure and the 5% damping ratio in the SEAOC/UBC design spectra. Details of this modification are presented in section 5.

The response spectrum analysis was performed with simultaneous excitation of 100 percent of the ground motion in the most critical direction and 30 percent of the ground motion in the orthogonal axis as described in the SEAOC/UBC regulations. The effective stiffness of the isolation system was modeled in ETABS by four short columns with identical properties and spaced appropriately as to match the rotational properties of the 45 isolators. Each column had one quarter the effective stiffness of the entire isolation system in the transverse and longitudinal directions.